Int. J. Environ. Res., 10(4):543-554, Autumn 2016
ISSN: 1735-6865

Modelling and Optimization of Homogenous Photo-Fenton Degradation of Rhodamine B by Response Surface Methodology and Artificial Neural Network

Speck, F., Raja, S.*, Ramesh, V. and Thivaharan, V.

Department of Biotechnology, Manipal Institute of Technology, Manipal, Karnataka, 576104, India

Received 2 July 2016; Revised 3 Sep. 2016; Accepted 10 Sep. 2016

ABSTRACT: The predictive ability of Response Surface Methodology (RSM) And Artificial Neural Network (ANN) in the modelling of photo-Fenton degradation of Rhodamine B (Rh-B) was investigated in the present study. The dye degradation was studied with respect to four factors *viz*., initial concentration of dye, concentration of H_2O_2 and Fe^{2+} ions and process time. Central Composite Design (CCD) was used to evaluate the effect of four factors and a second order regression model was obtained. The optimum degradation of 99.84% Rh-B was obtained when 159 ppm dye, 239 ppm H_2O_2, 46 ppm Fe^{2+} were treated for 27 min. The independent variables were fed as inputs to ANN with the percentage dye degradation as outputs. For the optimum percentage dye degradation, a three-layered feed-forward network was trained by Levenberg-Marquardt (LM) algorithm and the optimized topology of 4:10:1 (input neurons: hidden neurons: output neurons) was developed. A high regression coefficient ($R^2 = 0.9861$) suggested that the developed ANN model was more accurate and predicted in a better way than the regression model given by RSM ($R^2 = 0.9112$).

Key words: Photo-Fenton process, Rhodamine B degradation, Response surface methodology, Artificial Neural Network

INTRODUCTION

Production and dyeing of clothes are one of the important commercial activities in many Asian countries. However, a huge amount of chemical and biochemical waste are produced in these processes. The literature reveals that more than 100,000 different dyes are available and $7x10^5$ tons of dyestuffs are produced every year (Robinson et al., 2001). Substantial amount of them are released in textile coloration process which presents the main cause of pollution (Pearce et al., 2003; Kariyajjanavar et al., 2012). Dyes are mainly divided into acidic, basic, direct and reactive dyes. They have delocalized electron systems with conjugated double bonds, a chromophore as well as an auxochrome group (Rangabhashiyam et al., 2013). They are produced to be highly stable against many chemicals and natural conditions (Guimaraes et al., 2012). The molecular structure and the synthetic origin not only makes them difficult to decolorize but also highly water-soluble (Baldev et al., 2013). Most of the dye effluents are hard to treat, high in volume and contains harmful chemicals. They exhibit toxic and carcinogenic effects on biological systems and reduce the photosynthesis due to the absorbance of light that enters the water.

*Corresponding author E-mail:rajaselvaraj@gmail.com

Rhodamine B (Rh-B), one of the most important stable xanthene dyes, is also known as Basic Violet 10, and used in the textile industry for colouring (Baldev et al., 2013). Unfortunately, it is harmful for aquatic communities and also causes irritation of the skin and eyes (Nagaraja et al., 2012). Moreover, this dye is carcinogenic, neurotoxic and has a potential chronic toxicity towards humans, which makes it necessary to find a reasonable way of degrading Rh-B from aqueous solutions (Torrades and García-Montaño, 2014).

Many different ways of treating dye-containing wastewater have been studied so far, like coagulation, flocculation, foam flotation, membrane filtration and biological treatment. These methods differ in their efficiency, cost and environmental impact (Torrades and García-Montaño, 2014). One the most effective processes of degradation of dye in textile effluents is advanced oxidation processes (AOP) which includes photolysis, Fenton and photo-Fenton processes. All these methods depend on the formation of hydroxyl radicals (OH•) which have high oxidative power.

The Fenton's reagent consists of ferrous sulphate ($FeSO_4$) as a homogenous catalyst and hydrogen

peroxide (H_2O_2) as an oxidation agent. The conventional Fenton process is based on the formation of OH• radicals by electron transfer (Eq. 1) (Basturk and Karatas, 2014). These in-situ produced radicals initiate the non-selective destruction of the organic pollutants by attacking the unsaturated dye molecule and destroying the chromophores (Eq. 2-3) (Gan and Li, 2013; Siddique et al., 2014).

$$Fe^{2+} + H_2O_2 \rightarrow Fe^{3+} + OH^- + OH\bullet \quad (1)$$

$$OH\bullet + \text{organic dye} \rightarrow \text{intermediates} \quad (2)$$

$$OH\bullet + \text{intermediates} \rightarrow CO_2 + H_2O + \text{mineralization products} \quad (3)$$

The major setback of Fenton reaction is the accumulation of Fe^{3+} ions and the reaction does not proceed further, once all the Fe^{2+} ions are consumed. On the other hand, in photo-Fenton process, Fe^{3+} ions can react with water in the presence of UV radiation and can regenerate Fe^{2+} by photoreduction (Eq. 4). The newly generated Fe^{2+} can react with H_2O_2 and generate other free hydroxyl radicals as per Eq.1 and the cycle continues (Torrades and García-Montaño, 2014).

$$Fe^{3+} + H_2O + h\nu \rightarrow Fe^{2+} + H^+ + OH\bullet \quad (4)$$

The major setback of Fenton reaction is the accumulation of Fe^{3+} ions and the reaction does not proceed further, once all the Fe^{2+} ions are consumed. On the other hand, in photo-Fenton process, Fe^{3+} ions can react with water in the presence of UV radiation and can regenerate Fe^{2+} by photoreduction (Eq. 4). The newly generated Fe^{2+} can react with H_2O_2 and generate other free hydroxyl radicals as per Eq.1 and the cycle continues (Torrades and García-Montaño, 2014).

Therefore the photo-Fenton process generates many OH•, which increases the rate of degradation of pollutants as compared to the conventional Fenton process (Babuponnusami, and Muthukumar, 2014). The effectiveness of photo-Fenton process depends on many factors such as pH, temperature, source of light, the initial dye concentration, the concentration of H_2O_2 and Fe^{2+}. Therefore, it is essential to optimize the process by using specific optimization tools. In recent times, the use of response surface methodology (RSM) and artificial neural network (ANN) are gaining importance for modelling and optimization of many environmental processes (Kasiri et al., 2008, Noori et al., 2011 and Noori et al., 2013) Both the models estimate the relationship between the input factors and output responses of a process using the experimental values. Finally, the models are used to estimate the optimum conditions of the process (Marchitan et al., 2010).

In the literature, RSM has been applied for Rh-B dye degradation using sono-catalytic process (Pang et al., 2011) and heterogeneous Fenton-like catalyst system (Xu et al., 2013). However, it is evident from the existing literature that there are no reports dealing with the comparison of RSM and ANN modelling for the Rh-B dye degradation by photo-Fenton process.

Therefore, the objectives of the present investigation are (1) optimizing of the degradation of Rh-B by photo-Fenton process using RSM by taking four factors *viz*., concentration of Rh-B, H_2O_2, Fe^{2+} and time; (2) developing an ANN model and predicting the output of the photo-Fenton process.

MATERIALS & METHODS

(a) Chemicals: Analytical-grade Rhodamine B (C.I. Basic Violet 10) was used without any further purification and purchased from Hi Media, India. H_2O_2 and $FeSO_4.7H_2O$ were purchased from Merck. The required stock solutions of each component were prepared with Millipore-Milli-Q water.

(b) Photo-Fenton experiments: All the photo-Fenton experiments were performed in 25 ml beakers under room temperature. The samples were put in a UV Cabinet (Rotek Instruments, 230 V, 40 W, B&C Industries, Kerala, India) and irradiated with short wavelength of λ = 254 nm. For the determination of the degradation of dyes, UV/Vis measurements were performed at the absorbance maximum of λ = 552 nm using the UV/Vis spectrometer UVmini-1240 (UV-VIS Spectrometer, Shimadzu, Kyoto, Japan) at regular time intervals. Initially a dilution series was prepared to plot a calibration graph of Rh-B concentration versus absorbance.

(c) Experimental design by RSM: With a view to investigate the influence of the concentration of Rh-B, H_2O_2, Fe^{2+} and time on the degradation of Rh-B, a central composite design (CCD), which is one of the response surface methodologies, was used. Based on the previous experimental results, the levels of each factor were chosen and the values with both coded and uncoded forms are shown in the Table 1.

A total number of 30 experimental runs with different arrangements of levels of each factor are shown in Table 2. It consists of 16 factorial runs (2^4 full factorial), 8 axial runs (at a distance of $\alpha = \sqrt[4]{2^4} = 2$ from the centre) and 6 centre point runs to estimate the quadratic effect of variables on the response. The effects of extraneous factors were avoided by

conducting all the experiments in a random order (Montgomery, 2008).
The percentage dye degradation (% Y) was calculated by using

$$\% Y = 100 * (C_o - C_f) / C_o \quad (5)$$

where C_o and C_f are the initial and final concentrations of Rh-B respectively. After the completion of the experiments, the percentage dye degradation, Y was taken as the response and regression analysis was done to fit into a second order polynomial equation.

$$Y = \beta_0 + \sum_{i=1}^{k}(\beta_i \cdot x_i) + \sum_{i=1}^{k}(\beta_{i,i} \cdot x_i^2) + \sum_{i=1}^{k} \sum_{j=i+1}^{k}(\beta_{i,j} \cdot x_i \cdot x_j) + \epsilon \quad (6)$$

β_i: regression coefficient, x_i: factors, ϵ: error

The coefficients of this equation were calculated by the method of least squared error analysis. The statistical significance of the model and coefficients were checked by analysis of variance (ANOVA) (Wang and Wan, 2009a). The design and analysis of the experimental runs were performed with the statistical package software, Design Expert 7.0.0.

The coefficients of this equation were calculated by the method of least squared error analysis. The statistical significance of the model and coefficients were checked by analysis of variance (ANOVA) (Wang and Wan, 2009a). The design and analysis of the experimental runs were performed with the statistical package software, Design Expert 7.0.0.

(d) Modelling using ANN: ANN is a branch of artificial intelligence which is used to solve challenging problems like classification (speech recognition), forecasting, and optimization or multivariate data analysis using experimental data, field observations or even incomplete or fuzzy data sets (Kalogirou, 1999) . It can provide accurate solutions for highly complex and non-linear problems with many interrelating parameters and has therefore a better modelling ability than RSM (Basheer and Hajmeer, 2000). ANN has been already successfully used for many environmental applications (Noori et al., 2010a & 2010b).

The general network architecture of ANN is described by an input layer (IPL) receiving data, one or more hidden layers (HL) and output layer (OPL) presenting the desired response. Weights connect the neurons of the layers as well as storing the knowledge. Biases are not connected to the IPL, but are able to influence the hidden neurons independently and serve as a threshold. The net input is passed forward from the IPL to the HL and is processed by the neurons in the HL using a transfer function, e.g. linear, binary or sigmoid. The same procedure applies for the transfer of data from the HL to the OPL (Wang and Wan, 2009b). Before a network can be used for reproduction of data or optimization of processes, it has to be trained by presenting input data and targets. To learn the interrelationship between the input parameters and the output, the weights are modified in a certain way until the desired output is given (Wang and Wan, 2009b). This modification is done by a suitable learning method which defines how the weights should be adjusted. In this study, a 'feed-forward error-back propagation' algorithm has been employed. In this method, each iteration is composed of forward activation to produce a solution and the backward propagation of the calculated error to adjust the weights. The mean squared error (MSE) is propagated backwards from the OPL through the HL to the IPL, modifying the interconnecting weights. Thus, the validation is used to measure generalization of the network and stop the training, when no further improvement of generalization is noticed. During the third part, the testing, unused data is supplied to the network. When the MSE reaches the desired value, the training process is stopped. Together, the optimum weights matrices and bias matrices define the newly created ANN.

The experimental data obtained from the CCD matrix were used to train, test and validate the ANN model. The ANN modelling was executed with MATLAB 2013a (The Mathworks Inc., USA). The prediction accuracy and the degree of fitness of the

Table 1. Actual and coded levels of factors of the CCD experiments

Factor	Variables	Unit	Coded levels				
			-2	-1	0	1	2
A	Dye concentration	ppm	50	100	150	200	250
B	Hydrogen peroxide concentration	ppm	75	150	225	300	375
C	Fe^{2+} concentration	ppm	20	30	40	50	60
D	Time	min	3	12	21	30	39

ANN model were evaluated by calculating the following factors (Eq. 7 – 10) *viz.*, Mean Square Error (MSE), Root Mean Square Error (RMSE), Standard Error of Prediction (SEP), Average Absolute Relative Deviation (AARD).

$$MSE = \frac{\sum_{i=1}^{n}[Y_{i,exp} - Y_{i,pred}]^2}{n} \quad (7)$$

$$RMSE = \sqrt{\frac{\sum_{i=1}^{n}[Y_{i,exp} - Y_{i,pred}]^2}{n}} \quad (8)$$

$$SEP\ (\%) = 100 * \frac{RMSE}{Y_{ave}} \quad (9)$$

$$AARD(\%) = 100 * \frac{\sum_{i=1}^{n}\left[\left|\frac{Y_{i,exp} - Y_{i,pred}}{Y_{i,exp}}\right|\right]}{n} \quad (10)$$

RESULTS & DISCUSSIONS

(a) Modelling of dye degradation using RSM: A total number of 30 experiments were performed according to the CCD matrix to investigate the photo-Fenton process. Each of the experimental runs in the design matrix was unique which represented a specific combination of the four independent factors *viz.*, dye Fe^{2+} concentration, H_2O_2 concentration and time, with five different levels. For each experiment, the response (percentage degradation, %Y) was calculated and shown in the Table 2. The levels were coded since the variables had different units and limits (Göb et al., 1999). The last 6 runs were exactly the same, in order to account for the experimental error. The results of the experiments were used, together with the input data, to explore the relationship between dependent variables and the output. With the help of RSM, the following second order regression model (Eq. 11) was obtained. The regression model, however, was only valid in the range of experimental factor levels (50 < c (Rh B) < 250 ppm; 75 < c (H2O2) < 375 ppm; 20 < c (Fe2+) < 60 ppm; 3< time < 39 min).

(11)

$$Y = 95.7 - 4.77*A + 1.16*B + 7.91*C + 7.43*D + 0.36*A*B + 3.33*A*C + 1.87*A*D + 0.27*B*C + 0.56*B*D - 4.87*C*D + 0.41*A^2 - 0.05*B^2 - 3.77*C^2 - 4.87*D^2$$

The coefficients' significance was tested by student's t-test and the accuracy of the regression model was evaluated by ANOVA (Table 3).

The analysis was done at 95% confidence interval. The model F-value of 10.99 and $p < 0.0001$ implied the significant model attainment. There was only a 0.01% chance that a model F-value could occur due to noise. Moreover, $P < 0.05$ indicates the significant model terms. In this case, the linear terms A, C, D, the interaction terms AC, CD, and the quadratic terms C^2 and D^2 were significant model terms.

In general, for a satisfactory highly correlated model, the range of correlation coefficient R^2 should lie between 0.9 and 1. In the present study the R^2 of the model was 0. 9111 which indicated that 91.11% of the experimental data and predicted data can be explained by the model and thus confirmed the significance of the model. According to (Sohrabi et al., 2014), the coefficient of variation, CV should not be greater than 10% for a model to be reproducible. The CV obtained in this study was 6.42 %, which indicated precision and reliability of the results. Another important parameter is the adequate precision, which measures the signal-to-noise ratio. The value of 12.461 in this study indicated an adequate signal, which should be greater than 4 for a desirable model. Fig 1 indicates the goodness-of-fit model using the predicted and actual values of the RSM model, where the R^2 was 0.9112.

The interactive effect between the four variables on dye degradation was studied by examining the three-dimensional response surface plots (Fig 2). The 3D plots were constructed against two variables while keeping the remaining variables at their corresponding mid-value. The concave curved surfaces in the figures indicate the possibility of obtaining a maximum value within the levels chosen. It also confirms the interaction between the factors and the correctness of a second-order regression model.

Fig.2a shows the dependency of dye degradation on Fe^{2+} and dye concentration. While plotting this graph, H_2O_2 and time were maintained in their mid-levels. When the dye concentration was increased from low (50 ppm) to high concentration (250 ppm), the percentage of dye degradation decreased at the low level of Fe^{2+} (20 ppm). This could be due to the lesser amount of hydroxyl free radicals formed, to degrade the large number of dye molecules (Sohrabi et al., 2014; Tamimi et al., 2008). However, at the high level of Fe^{2+} (60 ppm), the degradation percentage did not have a significant effect. This remained at a high value which may be due to the saturation of Fe^{2+} ions. The fact that the increase in degradation percentage at lower Fe^{2+} concentration and remaining constant at a higher Fe^{2+} concentration reinforced the interaction between the concentration of Fe^{2+} and dye. This was further supported by the value of P which was less than 0.05. Fig. 2b shows the dependency of dye degradation on Fe^{2+} concentration and time. The plot was constructed by maintaining H_2O_2 and dye concentrations at their mid-levels. When the time was increased from 3 to 39

Table 2. Experimental design matrix and response based on experimental runs and predicted values by CCD andANN

Exp.No:	Factor Level				Response, Y (%)		
	A	B	C	D	Expt.	CCD	ANN
1	-1	-1	-1	-1	84.25	77.19	84.25
2	1	-1	-1	-1	59.05	56.52	59.05
3	-1	1	-1	-1	84.05	77.15	84.05
4	1	1	-1	-1	58.11	57.91	59.91
5	-1	-1	1	-1	98.6	95.56	98.60
6	1	-1	1	-1	91.65	88.23	91.65
7	-1	1	1	-1	98.9	96.59	96.75
8	1	1	1	-1	93.25	90.68	93.25
9	-1	-1	-1	1	97.15	96.95	97.54
10	1	-1	-1	1	83.65	83.76	83.65
11	-1	1	-1	1	97.91	99.13	97.91
12	1	1	-1	1	87.11	87.38	87.11
13	-1	-1	1	1	97.83	95.83	97.83
14	1	-1	1	1	91.85	95.98	91.85
15	-1	1	1	1	99.32	99.08	99.32
16	1	1	1	1	95.81	100.67	95.81
17	-2	0	0	0	99.11	106.89	101.56
18	2	0	0	0	90.62	87.81	86.95
19	0	-2	0	0	88.64	93.16	93.80
20	0	2	0	0	97.35	97.80	97.35
21	0	0	-2	0	59.62	64.77	62.41
22	0	0	2	0	96.61	96.43	96.61
23	0	0	0	-2	49.83	61.36	49.83
24	0	0	0	2	97.65	91.09	97.65
25	0	0	0	0	92.21	95.70	95.19
26	0	0	0	0	96.35	95.70	95.19
27	0	0	0	0	96.7	95.70	95.19
28	0	0	0	0	96.55	95.70	95.19
29	0	0	0	0	96.82	95.70	95.19
30	0	0	0	0	95.55	95.70	95.19
AARD (%)						3.66	1.07
RMSE						4.04	1.62
SEP (%)						4.54	1.82

Table 3. ANOVA table for RSM model

Source	Coefficient	Sum of squares	DF	Mean square	F value	P value
Model	95.69667	5029.701	14	359.2644	10.99313	< 0.0001*
A	-4.77125	546.3558	1	546.3558	16.71795	0.0010*
B	1.160417	32.3176	1	32.3176	0.988887	0.3358
C	7.912917	1502.742	1	1502.742	45.98242	< 0.0001*
D	7.43375	1326.255	1	1326.255	40.5821	< 0.0001*
AB	0.358125	2.052056	1	2.052056	0.062791	0.8055
AC	3.334375	177.8889	1	177.8889	5.443224	0.0340*
AD	1.871875	56.06266	1	56.06266	1.715462	0.2100
BC	0.266875	1.139556	1	1.139556	0.034869	0.8544
BD	0.556875	4.961756	1	4.961756	0.151825	0.7023
CD	-4.87188	379.7627	1	379.7627	11.62036	0.0039*
A^2	0.413229	4.683657	1	4.683657	0.143315	0.7103
B^2	-0.05427	0.080786	1	0.080786	0.002472	0.9610
C^2	-3.77427	390.7233	1	390.7233	11.95575	0.0035*
D^2	-4.86802	649.9921	1	649.9921	19.88911	0.0005*
Residual		490.212	15	32.6808		
Cor Total		5519.913	29			

* significant at 95% confidence interval
SD: 5.72; R2: 0.9111; Adeq. Precision: 12.4605 ; C.V.%: 6.42

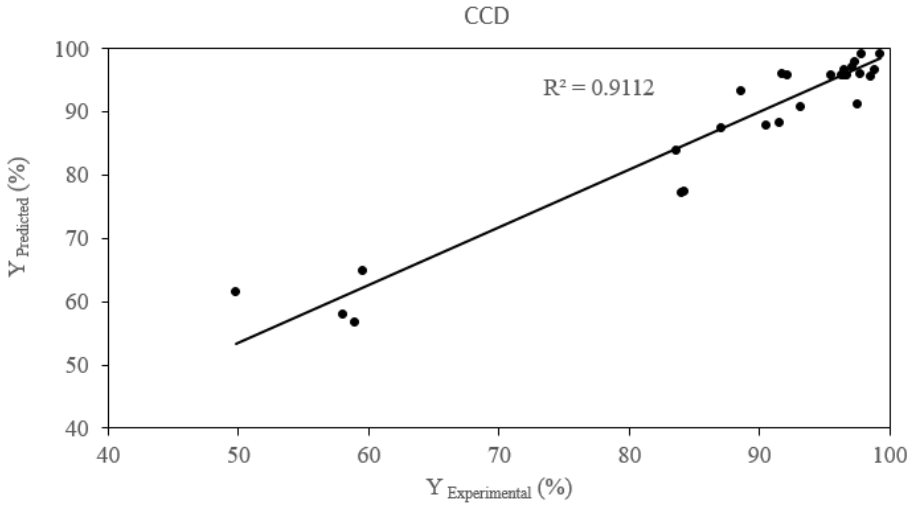

Fig. 1. Scatter plot of predicted vs experimental % dye degradation from RSM model

min, the dye degradation percentage increased at the low level of Fe^{2+} (20 ppm). However, at the high level of Fe^{2+} (60 ppm), the degradation % increased till 21 min and further increase in time decreased the degradation percentage. Since the effect of time relied on the level of Fe^{2+}, these two show significant interactions (low P value of 0.0039). The decrease in percentage dye degradation may be caused by scavenging of free OH• free radicals (Torrades and García-Montaño, 2014) by the high concentration of Fe^{2+} to form Fe^{3+} (Eq. 12), which resulted in the UV light absorption and caused the recombination of OH• free radicals (Ebrahiem et al., 2013).

$$Fe^{2+} + OH\bullet \rightarrow Fe^{3+} + OH^- \quad (12)$$

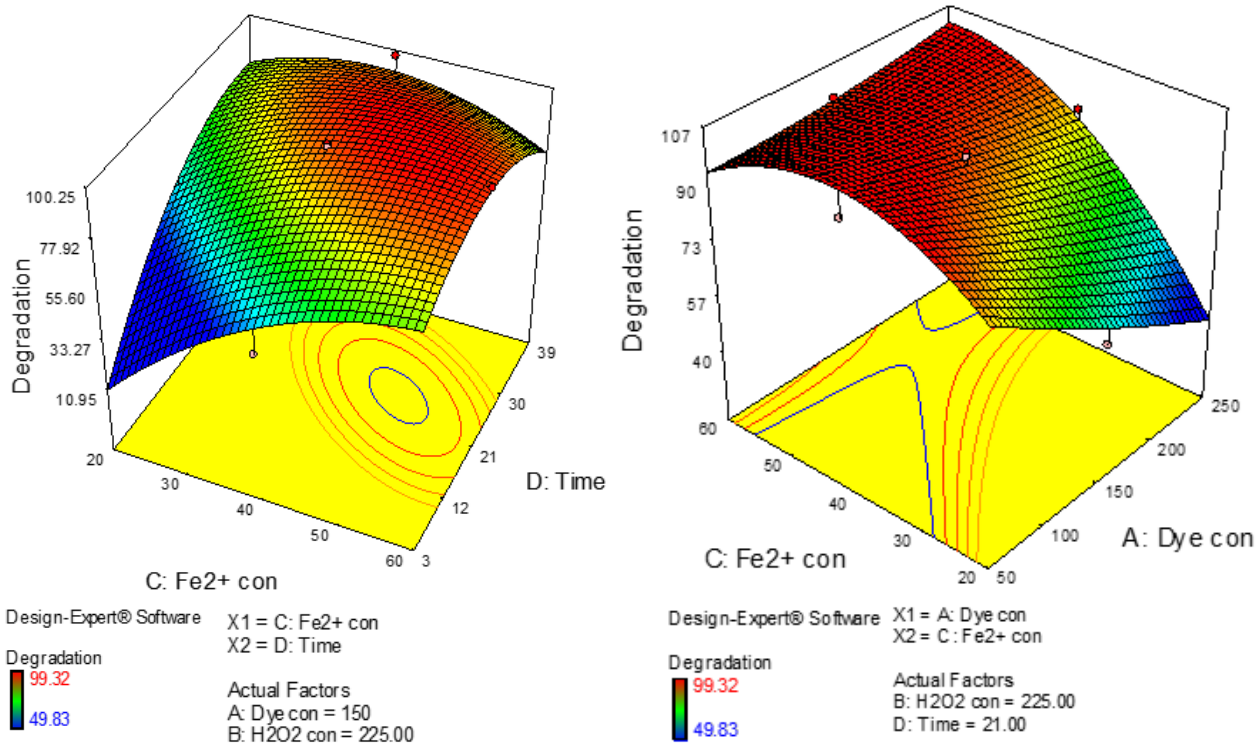

Fig. 2. Response surface plots (a) Interaction plot of Fe^{2+} concentration and Dye concentration (b) Interaction plot of Fe^{2+} concentration and Time

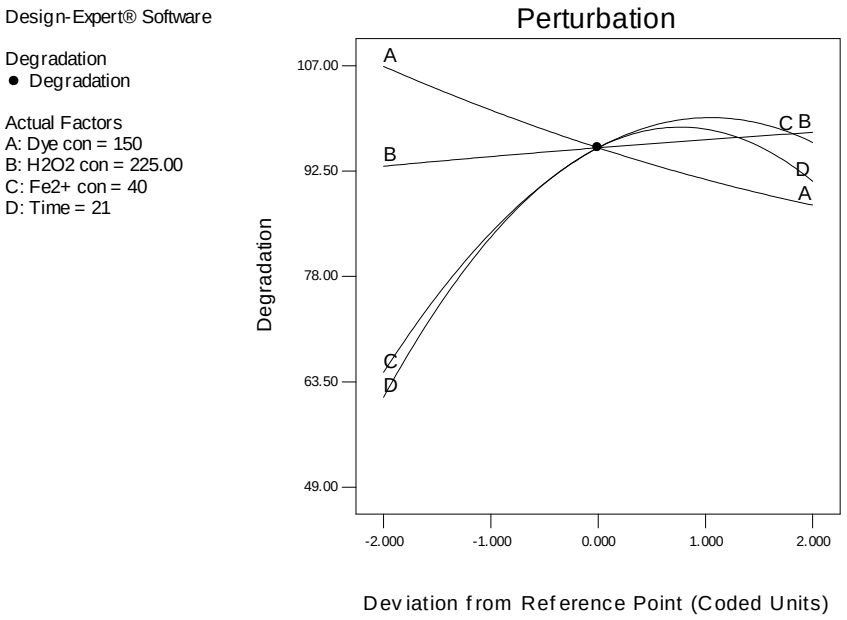

Fig. 3. Perturbation plot showing the effect of variables on % Dye degradation

Fig. 3 shows the perturbation plot, which gives the comparative effects of the variables on dye degradation. This plot shows the variation in the output as each factor changes from a chosen reference point while the remaining factors are kept constant at the reference point. A substantial slope or curvature in a factor implies that the output is very sensitive to the change in the factor (Kalariya et al., 2014). In the present study, the steep curvature in C (Fe^{2+}) and D (time) curves showed that the dye degradation was very sensitive to these variables. Curve A (dye concentration) was less sensitive when compared to

curves C and D. A flat profile for factor B (H_2O_2) indicated that it had no sensitivity towards the response. Therefore the most significant factor in the dye degradation was Fe^{2+} followed by time and dye concentration. This fact was corroborated by the absolute values of the coefficients of linear terms as given in Table 3, which followed the order: C > D > A > B. In addition to these, the least sensitive factor B was not significant (P > 0.05) whereas the other factors A, C and D were significant (P<0.05).

In order to find out the optimum percentage dye degradation, the second order regression equation was solved by using the desirability function (Satapathy and Das, 2014) and the conditions for a desirability of 1 were as follows: Dye concentration – 159.27 ppm; H_2O_2 concentration – 239.21 ppm; Fe^{2+} concentration – 46.18 ppm; Time – 27.29 min and the predicted % dye degradation – 99.95%. Confirmatory experiments were done with dye concentration – 159 ppm; H_2O_2 concentration – 239 ppm; Fe^{2+} concentration – 46 ppm and time – 27 min and the calculated % dye degradation were found to be 99.84%, which was close to the predicted value. The degradation process at optimized conditions is shown in Fig 4. It can be noticed from the figure that the characteristic peak of Rhodamine B, λ = 552 nm disappears at the end of the photo-Fenton process which confirms the complete degradation of dye. The visual images of the degradation process are also shown in the Fig 4.

(b) Modelling of dye degradation using ANN: For analysing and modelling the photo-Fenton process of the degradation of Rh-B, artificial neural network was used. The crucial step in ANN is the selection of network size, the number of hidden layers and hidden neurons. The CCD data set was used to create a network model with an IPL, one HL and an OPL. The experimental data was divided into three categories, namely, training (70%), validation (15%) and testing (15%). The performance of the trained model against new data was checked the testing set. The results of this set provided an independent measure of the performance of the ANN model, during and after training (Lin et al., 2008).

The network was trained using Levenberg-Marquardt back-propagation algorithm (Elmolla et al., 2010). A hyperbolic tangent sigmoid transfer function (*tansig*) was employed for processing the data in the HL and a linear transfer function (*purelin*) was used to determine the effect of the values on the output nodes. The connections between the different layers and neurons were represented by weights and biases. IW and HW represented the input and HL weight matrices, respectively. Ib and Ob represented the biases of input and OPL respectively. The training was stopped when MSE reached a minimum (Sabzevari and Moosavi, 2014) and the optimum values for weights and biases were saved to define the ANN model. The optimal number of hidden neurons was determined by adding neurons during the training and comparing the R^2, MSE and AARD of each network (Table 4).

Since MSE, R^2 as well as AARD % values has reached a minimum for 10 hidden neurons, the optimum number of neurons in the HL is 10. Therefore, the selected topology of ANN in the present study

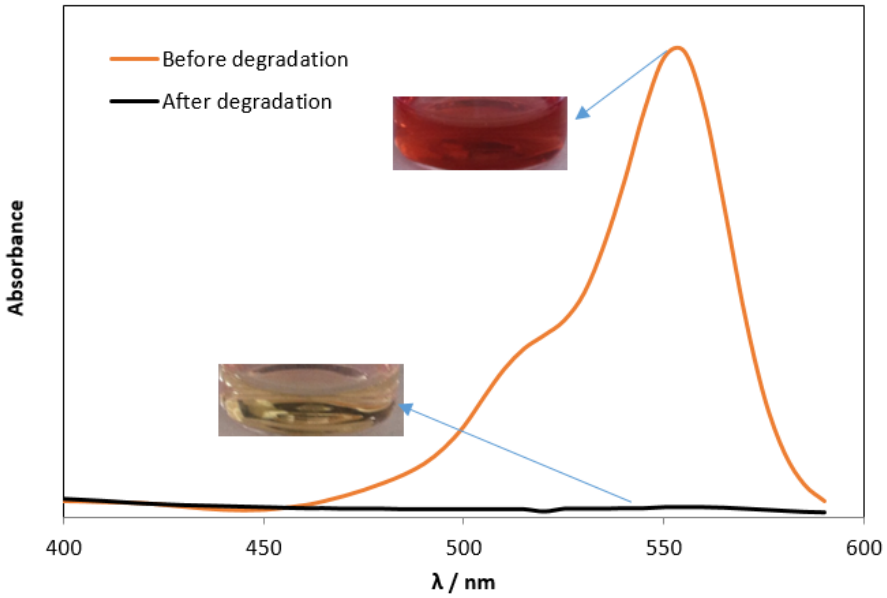

Fig. 4. Absorption spectra of Rhodamine B before and after the degradation by photo-Fenton process at optimized conditions

consisted of 4 input neurons, 10 hidden neurons and one output neuron (4:10:1). The optimal structure of the ANN model in this study is shown in Fig. 5 and the optimized weights and biases of the developed model are given in Table 5.

The ANN model developed for the prediction of % dye degradation was being described using the inputs X_i and the output Y (Sathish, and Prakasham, 2010) as:

$$Y = purelin\,(HW * tansig\,(IW) * X_i' + Ib) + Ob) \quad (14)$$

Table 4. Results of topology studies to find the optimal ANN configuration

Number of Hidden neurons	Error Analysis		
	R^2	MSE	AARD (%)
4	0.93	27.1848	3.353516
8	0.98	8.879109	1.751032
10	**0.99**	**2.63**	**1.071695**
12	0.97	13.3162	2.358209
14	0.93	36.98525	5.444711

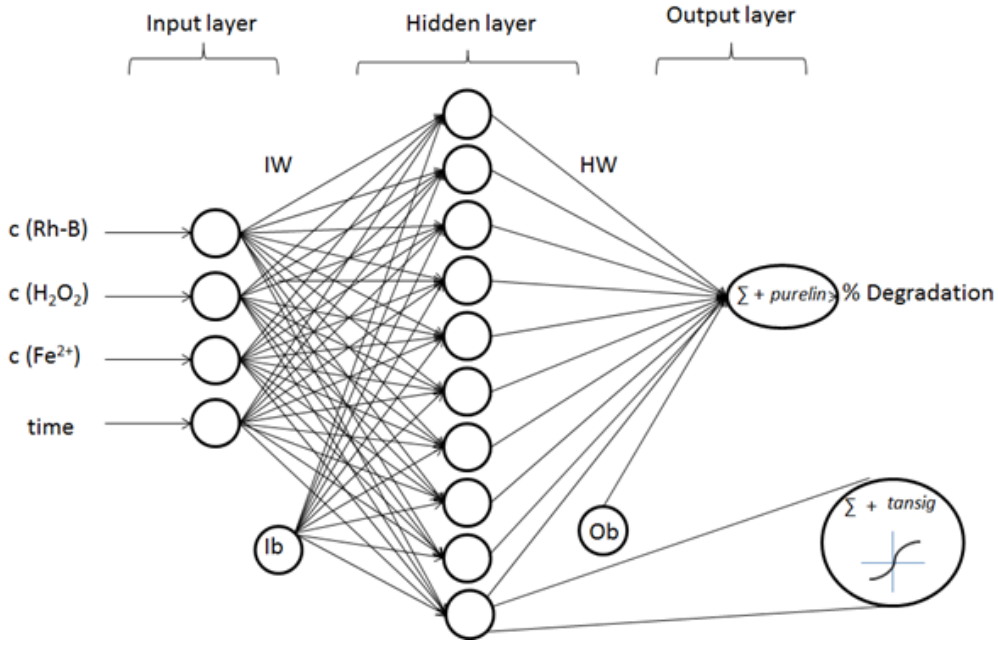

Fig. 5. Structure of ANN model used for the prediction of % Dye degradation

Table 5. Optimum values of weight matrices and biases resulting from ANN model

IW				HW	Ib	Ob
1.4258	1.0306	-0.2585	1.398	-0.1788	-2.719	-1.2497
1.4985	-0.3544	-3.6242	-1.8194	-0.7187	-2.4961	
-0.7666	-1.5137	-1.2355	-0.6316	-0.0511	1.1378	
3.8551	-1.6939	-0.8707	-0.6713	-0.1726	-0.0718	
-3.9187	0.3368	0.3455	-0.539	-0.5289	-0.3498	
2.8403	-0.0095	-0.1156	0.5739	-0.5609	0.4198	
1.883	-1.7552	0.2922	0.1536	0.0048	0.8872	
0.661	-0.9254	0.4194	3.943	1.4968	3.9616	
0.497	-2.3366	-0.653	-0.1522	-0.0477	2.0206	
-1.6979	0.1736	-1.4078	0.2699	0.1837	-2.8443	

By using the weights and biases, the output of the ANN model was calculated and given in Table 2. The low values of RMSE, AARD and SEP suggested that the model given by ANN was more accurate compared to the regression model of RSM. The correlation between the experimental values and the calculated responses from the ANN model for the % dye degradation is shown in Fig 6. The correlation coefficient of 0.9861 of the plot indicated the reliability of the ANN model in the system (Kýranþan et al., 2015).

In addition, the residual error (Maran and Priya, 2015) was calculated for both the models and it can be seen from the Fig. 7 that the deviation between experimental and predicted values of ANN model was very less as compared to the RSM model (Fig. 7).

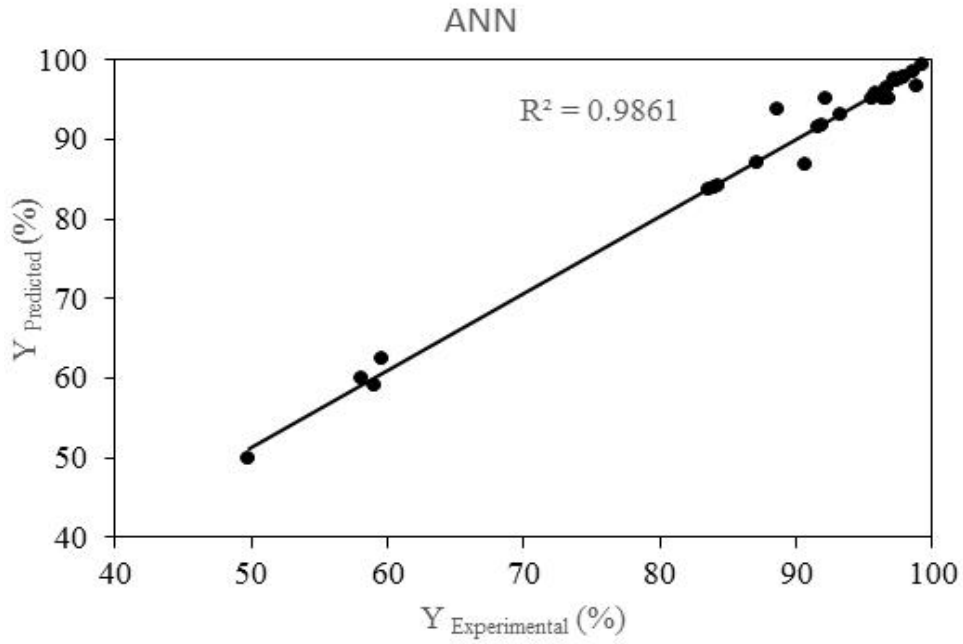

Fig. 6. Scatter plot of predicted vs experimental % dye degradation from ANN model

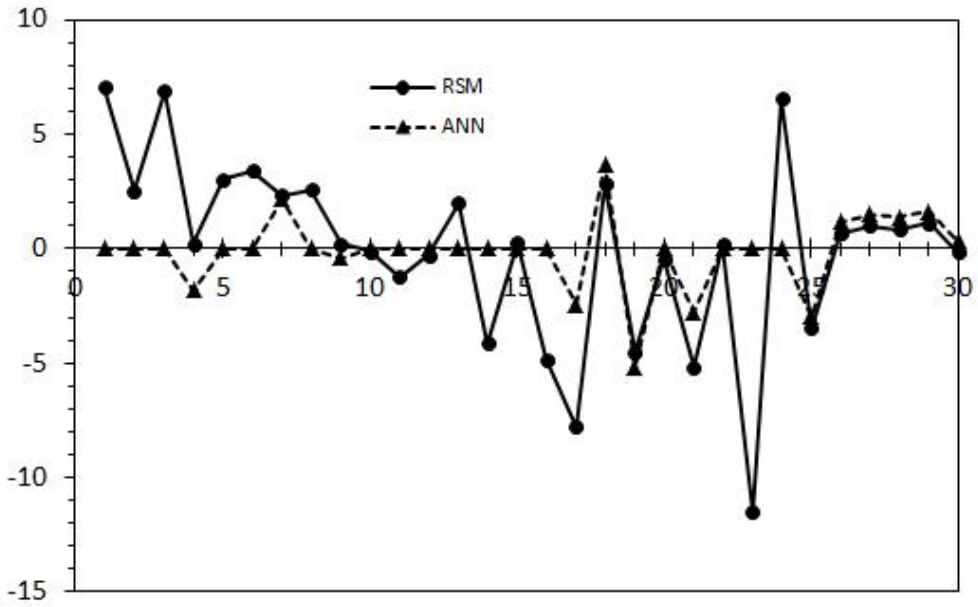

Fig. 7. Residual errors between predicted and experimental % dye degradation from RSM and ANN models

CONCLUSIONS

Photo-Fenton process was used to degrade Rh-B and the various process parameters such as initial concentration of dye, process time, concentration of H_2O_2 and Fe^{2+} ions were optimized by using response surface methodology, which gave a second-order regression equation. The optimum process conditions were found out to be initial dye concentration – 159 ppm; H_2O_2 concentration – 239 ppm; Fe^{2+} concentration – 46 ppm and Time – 27 min with 99.84% dye degradation. Both RSM and ANN models were in coherent with the experimental results. The low values of root mean square (RMSE), average absolute relative deviation (AARD) and standard error of prediction (SEP) suggested that the developed ANN model was more accurate compared to the regression model given by RSM. Therefore ANN could serve as a tool to accurately predict and model the dye degradation process.

ACKNOWLEDGMENTS

Franziska Speck is thankful to IAESTE (International Association for the Exchange of Students for Technical Experience) at Manipal University for being selected as an intern to work in this project. All the authors thank Department of Biotechnology, MIT, Manipal University.

REFERENCES

Babuponnusami, A. and Muthukumar, K. (2014). A review on Fenton and improvements to the Fenton process for wastewater treatment. Journal of Environmental Chemical Engineering, **2(1),** 557-572.

Baldev, E., MubarakAli, D., Ilavarasi, A., Pandiaraj, D., Ishack, K. S. S. and Thajuddin, N. (2013). Degradation of synthetic dye, Rhodamine B to environmentally non-toxic products using microalgae. Colloids and Surfaces B: Biointerfaces, **105,** 207-214.

Basheer, I. A. and Hajmeer, M. (2000). Artificial neural networks: fundamentals, computing, design, and application. Journal of microbiological methods, **43(1),** 3-31.

Basturk, E. and Karatas, M. (2014). Advanced oxidation of reactive blue 181 solution: A comparison between fenton and sono-fenton process. Ultrasonics sonochemistry, **21(5),** 1881-1885.

Ebrahiem, E. E., Al-Maghrabi, M. N. and Mobarki, A. R. (2013). Removal of organic pollutants from industrial wastewater by applying photo-Fenton oxidation technology. Arabian Journal of Chemistry., doi:10.1016/ j.arabjc.2013.06.012.

Elmolla, E. S., Chaudhuri, M. and Eltoukhy, M. M. (2010). The use of artificial neural network (ANN) for modeling of COD removal from antibiotic aqueous solution by the Fenton process. Journal of hazardous materials, **179(1),** 127-134.

Gan, P. P. and Li, S. F. Y. (2013). Efficient removal of Rhodamine B using a rice hull-based silica supported iron catalyst by Fenton-like process.*Chemical engineering journal*, ***229*,** 351-363.

Göb, S., Oliveros, E., Bossmann, S. H., Braun, A. M., Guardani, R. and Nascimento, C. A. (1999). Modeling the kinetics of a photochemical water treatment process by means of artificial neural networks. Chemical Engineering and Processing: Process Intensification, **38(4),** 373-382.

Guimaraes, J. R., Maniero, M. G. and de Araujo, R. N. (2012). A comparative study on the degradation of RB-19 dye in an aqueous medium by advanced oxidation processes. Journal of environmental management, **110,** 33-39.

Kalariya, P. D., Namdev, D., Srinivas, R. and Gananadhamu, S. (2014). Application of experimental design and response surface technique for selecting the optimum RP-HPLC conditions for the determination of moxifloxacin HCl and ketorolac tromethamine in eye drops. *Journal of Saudi Chemical Society*.

Kalogirou, S. A. (1999). Applications of artificial neural networks in energy systems. Energy Conversion and Management, **40(10),** 1073-1087.

Kariyajjanavar, P., Narayana, J. and Nayaka, Y. A. (2012). Degradation of Textile Wastewater by Electrochemical Method. Hydrology: Current Research, 2011.

Kasiri, M. B., Aleboyeh, H. and Aleboyeh, A. (2008). Modeling and optimization of heterogeneous photo-fenton process with response surface methodology and artificial neural networks. Environmental science and technology, **42(21),** 7970-7975.

Kıranþan, M., Khataee, A., Karaca, S. and Sheydaei, M. (2015). Artificial neural network modeling of photocatalytic removal of a disperse dye using synthesized of ZnO nanoparticles on montmorillonite. Spectrochimica Acta Part A: Molecular and Biomolecular Spectroscopy, **140,** 465-473.

Lin, C. C., Wang, Y. C., Chen, J. Y., Liou, Y. J., Bai, Y. M., Lai, I. C. and Li, Y. C. (2008). Artificial neural network prediction of clozapine response with combined pharmacogenetic and clinical data. Computer methods and programs in biomedicine, **91(2),** 91-99.

Maran, J. P. and Priya, B. (2015). Modeling of ultrasound assisted intensification of biodiesel production from neem (Azadirachta indica) oil using response surface methodology and artificial neural network. Fuel, **143,** 262-267.

Marchitan, N., Cojocaru, C., Mereuta, A., Duca, G., Cretescu, I. and Gonta, M. (2010). Modeling and optimization of tartaric acid reactive extraction from aqueous solutions: A comparison between response surface methodology and artificial neural network. Separation and Purification Technology, **75(3),** 273-285.

Montgomery, D. C. (2008). Design and analysis of experiments. John Wiley & Sons

Nagaraja, R., Kottam, N., Girija, C. R. and Nagabhushana, B. M. (2012). Photocatalytic degradation of Rhodamine B

dye under UV/solar light using ZnO nanopowder synthesized by solution combustion route. Powder technology, **215,** 91-97.

Noori, R., Karbassi, A. and Sabahi, M. S. (2010a). Evaluation of PCA and Gamma test techniques on ANN operation for weekly solid waste prediction. Journal of Environmental Management, **91(3),** 767-771.

Noori, R., Khakpour, A., Omidvar, B. and Farokhnia, A. (2010b). Comparison of ANN and principal component analysis-multivariate linear regression models for predicting the river flow based on developed discrepancy ratio statistic. Expert Systems with Applications, **37(8),** 5856-5862.

Noori, R., Karbassi, A. R., Mehdizadeh, H., Vesali Naseh, M. and Sabahi, M. S. (2011). A framework development for predicting the longitudinal dispersion coefficient in natural streams using an artificial neural network. Environmental Progress and Sustainable Energy, **30(3),** 439-449.

Noori, R., Karbassi, A. R., Ashrafi, K., Ardestani, M. and Mehrdadi, N. (2013). Development and application of reduced order neural network model based on proper orthogonal decomposition for BOD5 monitoring: Active and online prediction. Environmental progress & sustainable energy, **32(1),** 120-127.

Pang, Y. L., Abdullah, A. Z. and Bhatia, S. (2011). Optimization of sonocatalytic degradation of Rhodamine B in aqueous solution in the presence of TiO_2 nanotubes using response surface methodology. Chemical engineering journal, **166(3),** 873-880.

Pearce, C. I., Lloyd, J. R. and Guthrie, J. T. (2003). The removal of colour from textile wastewater using whole bacterial cells: a review. Dyes and pigments, **58(3),** 179-196.

Rangabhashiyam, S., Anu, N. and Selvaraju, N. (2013). Sequestration of dye from textile industry wastewater using agricultural waste products as adsorbents. Journal of Environmental Chemical Engineering, **1(4),** 629-641.

Robinson, T., McMullan, G., Marchant, R. and Nigam, P. (2001). Remediation of dyes in textile effluent: a critical review on current treatment technologies with a proposed alternative. Bioresource technology, **77(3),** 247-255.

Siddique, M., Farooq, R. and Price, G. J. (2014). Synergistic effects of combining ultrasound with the Fenton process in the degradation of Reactive Blue 19. Ultrasonics sonochemistry, **21(3),** 1206-1212.

Sohrabi, M. R., Moghri, M., Masoumi, H. R. F., Amiri, S. and Moosavi, N. (2014). Optimization of Reactive Blue 21 removal by Nanoscale Zero-Valent Iron using response surface methodology. Arabian Journal of Chemistry., doi:10.1016/j.arabjc.2014.11.060 .

Torrades, F. and García-Montaño, J. (2014). Using central composite experimental design to optimize the degradation of real dye wastewater by Fenton and photo-Fenton reactions. Dyes and pigments, **100,** 184-189.

Tamimi, M., Qourzal, S., Barka, N., Assabbane, A. and Ait-Ichou, Y. (2008). Methomyl degradation in aqueous solutions by Fenton's reagent and the photo-Fenton system. Separation and Purification Technology, **61(1),** 103-108.

Sabzevari, S. and Moosavi, M. (2014). Density prediction of liquid alkali metals and their mixtures using an artificial neural network method over the whole liquid range. Fluid Phase Equilibria, **361,** 135-142.

Satapathy, M. K. and Das, P. (2014). Optimization of crystal violet dye removal using novel soil-silver nanocomposite as nanoadsorbent using response surface methodology. Journal of Environmental Chemical Engineering, **2(1),** 708-714.

Sathish, T. and Prakasham, R. S. (2010). Enrichment of glutaminase production by Bacillus subtilis RSP GLU in submerged cultivation based on neural network—genetic algorithm approach. Journal of Chemical Technology and Biotechnology, **85(1),** 50-58.

Wang, J. and Wan, W. (2009a). Experimental design methods for fermentative hydrogen production: a review. International journal of hydrogen energy, **34(1),** 235-244.

Wang, J. and Wan, W. (2009b). Optimization of fermentative hydrogen production process using genetic algorithm based on neural network and response surface methodology. international journal of hydrogen energy, **34(1),** 255-261.

Xu, H. Y., Qi, S. Y., Li, Y., Zhao, Y. and Li, J. W. (2013). Heterogeneous Fenton-like discoloration of Rhodamine B using natural schorl as catalyst: optimization by response surface methodology. Environmental Science and Pollution Research, **20(8),** 5764-5772.